Supplementary information for

Photocatalytic degradation of ciprofloxacin in freshwater aquaculture wastewater by CNBN membrane: Mechanism, antibacterial activity, and cyclability

Zhenjun Xiao[a], Yixun Zheng[a], Ping Chen[a*], Haijin Liu[b], Zheng Fang[a], Junlong Zhang[c], Zifeng Lin[a], Yudan Zhang[a], Jin Luo[a], Weihong Zhang[a], Wenying Lv[a], Guoguang Liu[a*]

[a] School of Environmental Science and Engineering, Guangdong University of Technology, Guangzhou, 510006, China

[b] School of Environment, Key Lab Yellow River & Huaihe River Water Environment, Henan Normal University, Xinxiang, Henan, 453007, China

[c] Macao Environmental Research Institute, Macao University of Science and Technology, Macao, 999078, China

***Corresponding Author: Ping Chen; Guoguang Liu**

E-mail address: gdutchp@163.com; liugg615@163.com

Phone: +86-20-39322547, Fax: +86-20-39322548

Summary:

Number of pages: 30

Number of Texts: 4

Number of tables: 5

Number of figures: 13

Text S1. Method of CN' s preparation

6 g of melamine was added to an alumina crucible, then the alumina crucible was transferred to a muffle furnace and heated to 550°C at a steady rate of 3 °C min^{-1} for 4 hours. After cooling to room temperature, the obtained powder was transferred to an agate mortar for grinding and screening (100 mesh) to obtain the final material (CN).

Text S2. Method of HPLC-MS/MS detection.

The intermediates of CIP were Identified by a liquid chromatograph system (Ultimate 3000RSLC, Thermo Scientific; USA) equipped with Q Exactive Orbitrap precise mass spectrometer (Q Exactive, Thermo Scientific; USA). Separation of intermediate products was accomplished using an Agilent SB-C18 column (5 μm, 4.6× 150 mm). Flow rate of mobile phase was performed at 0.2 mL min^{-1} with H_2O. containing 0.2 % (v/v) formic acid, as eluent A, and methanol as eluent B. Program elution was employed by a linear gradient in the composition of the mobile phase. Mainly, the proportion of eluent B increased from 10 % to 60 % in 30 min, and then, from 60% to 100% (v/v) in the next 2 min.

Text S3. Method of photoluminescence spectra

The photoluminescence spectra were monitored with fluorescence spectrophotometer (F97 pro, Shanghai Lengguang; China).

Text S4. Method of H_2O_2 detection experiment.

Method of quantizing H_2O_2 was referred to Kormann et al. [1, 2]. Specifically, 1.5 mL reaction solution was sampled at a certain interval after being filtered by a 0.45 μm filter. Then 0.75 mL potassium phthalate and 0.75 mL potassium iodide reagent were added successively. Potassium iodide reagent was a mixture containing 0.4 M potassium iodide, 0.06 M sodium hydroxide and 10^{-4} M ammonium molybdate. Fifteen minutes after the sample was reacted with potassium iodide, the solution was measured by spectrophotometer at 350 nm, and the concentration of H_2O_2 can be calculated by the standard curve (Fig. S11). In order to make a more intuitive comparison of H_2O_2 generation in the reaction process, we established the following formula (Eqns. (S1-S2)) to reveal the generation rate, and verified the comparison and matching degree between the established formula and experimental data.

$$\triangle k_{fi} = \frac{dC_i}{dT_i} \qquad (\mathrm{Eq}n.\ S)$$

1.

$$\overline{k_f} = \frac{\sum_{i=0}^{n} \triangle K_{fi} \cdot T_i}{\sum_{i=0}^{n} T_i} \left(\times 10^{-6} M\ min^{-1} \right) \qquad \text{(Eq}n\text{. S2)}$$

In Eqns. 1-2, $\triangle k_{fi}$ represents the instantaneous generation rate of H_2O_2 ($\times 10^{-6} M\ min^{-1}$), $\overline{\frac{dC_i}{dT_i}}$ represents the first derivative of the instantaneous concentration of H_2O_2 with respect to time, T_i represents certain time, $\overline{k_f}$ represents the average rate of H_2O_2 production.

Table S1. Main water quality parameters for the freshwater aquaculture wastewater.

Parameters	Test method	Value
COD	Potassium dichromate method (GB11914-89, National environmental protection standard of the people's Republic of China)	216.2 mg L^{-1}
ammonia nitrogen	Nessler reagent spectrophotometry (HJ 535-2009, National environmental protection standard of the people's Republic of China)	20.3 mg L^{-1}
pH	pH meter	5.3

Table S2. Qualitative analysis result of freshwater aquaculture wastewater by ICP-MS.

Element	Concentration (ppm)
Be	0.000007
B	0.079316
Na	18.584414[#]
Mg	3.729475
Al	0.002111
k	21.110477
Ca	6.901739
Ti	0.133015
V	0.001348
Cr	0.000914
Mn	0.004137
Fe	0.175868
Co	0.000233
Ni	0.001045
Cu	0.001566
Zn	0.007099
As	0.003694
Se	0.000989
Mo	0.002168
Ag	0.000014
Cd	0.00001
Sb	0.000341
Ba	0.077954
Tl	0.000003
Pb	0.000274

[#] The red numbers represent cationic concentration reaches ppm level

Table S3. HPLC parameters of contaminants and probes.

Names	Mobile phase composition	Detection wavelength (nm)	Chromatographic Column	Column Temperature
Ciprofloxacin	Methanol :0.2% formic acid 30:70(v:v)	278	Zorbax Eclipse XDB-C18 （4.6×250mm）	35°C
Ofloxacin	Methanol :0.2% formic acid 25:75(v:v)	293	Zorbax Eclipse XDB-C18 （4.6×250mm）	35°C
Norfloxacin	Methanol :0.2% formic acid 25:75(v:v)	278	Zorbax Eclipse XDB-C18 （4.6×250mm）	35°C
Sulfamethazine	Methanol :0.2% formic acid 30:70(v:v)	262	Zorbax Eclipse XDB-C18 （4.6×150mm）	35°C
Sulfamethoxazole	Methanol :0.2% formic acid 30:70(v:v)	275	Zorbax Eclipse XDB-C18 （4.6×150mm）	35°C
Sulfisoxazole	Methanol :0.2% formic acid 40:60(v:v)	275	Zorbax Eclipse XDB-C18 （4.6×150mm）	35°C
Nitrobenzene	Acetonitrile :0.1% formic acid 55:45(v:v)	262	Zorbax Eclipse XDB-C18 （4.6×150mm）	30°C
Furfuryl alcohol	Acetonitrile: ultrapure water 50:50(v:v)	219	Zorbax Eclipse XDB-C18 （4.6×250mm）	35°C

Table S4. Information of transformation products during the degradation of CIP by CNBN membrane photocatalytic system under simulated sunlight irradiation.

Sequence number	Retention time (min)	$[M+H]^+$	Molecular weight (Da)	Structure
CIP	8.74	332.13995	331	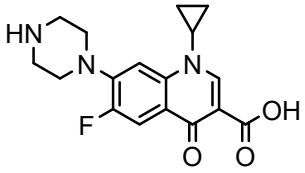
P1	14.59	318.29990	317	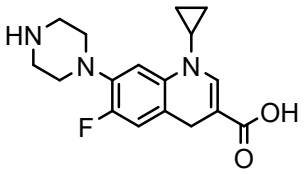
P2	14.84	290.26862	289	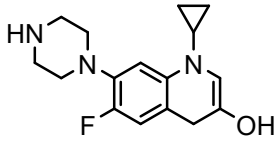
P3	14.73	274.27374	273	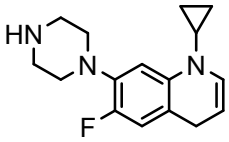
P4	17.64	256.26328	255	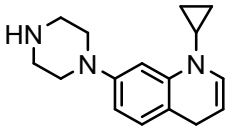
P5	9.50	362.11423	361	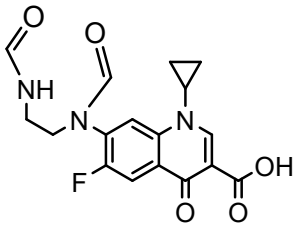
P6	8.50	344.22733	343	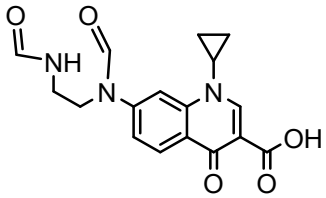
P7	14.86	334.29587	333	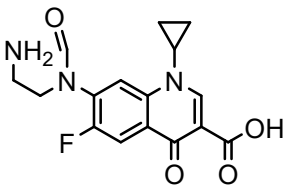

P8	13.49	334.29495	333	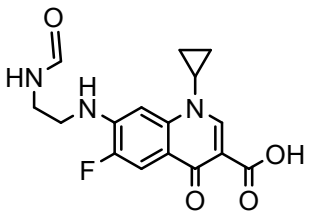
P9	8.37	306.12448	305	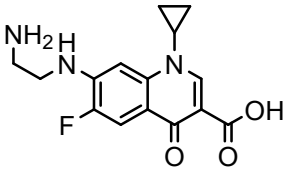
P10	16.35	304.29968	303	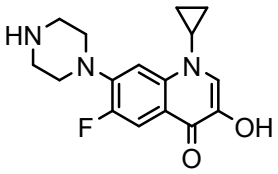
P11	13.87	263.05663	262	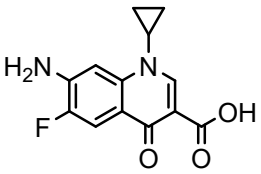
P12	16.85	279.22906	278	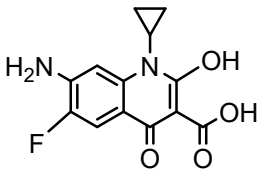
P13	12.87	227.16164	226	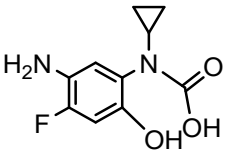
P14	9.68	245.13567	244	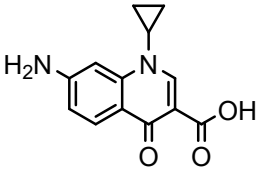
P15	8.95	205.09094	204	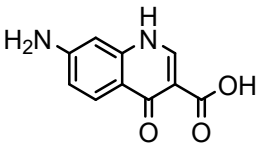
P16	13.05	293.17087	292	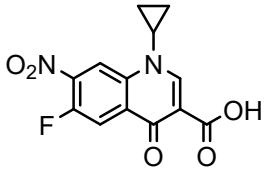

P17	10.06	279.07959	274	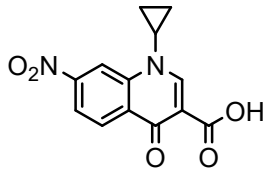

Table S5. Calculation results of frontier electron densities on atoms of CIP

Atom (number)[a]	$2FED^2_{HOMO}$	$FED^2_{HOMO}+FED^2_{LUMO}$	Point charge
N(1)	**0.43769**[b]	**0.23168**[c]	-
C(14)	-	-	**0.44870**
C(15)	-	**0.26899**	-
N(4)	**0.19448**	-	-
C(22)	-	-	**0.42240**
C(12)	-	-	**0.37663**

a: See Figuge. S9 in the SI for atomic numbering.

b: The calculation results of electron density on atoms of CIP are referenced from our group's previous research [3].

c: Significant values are highlighted with color.

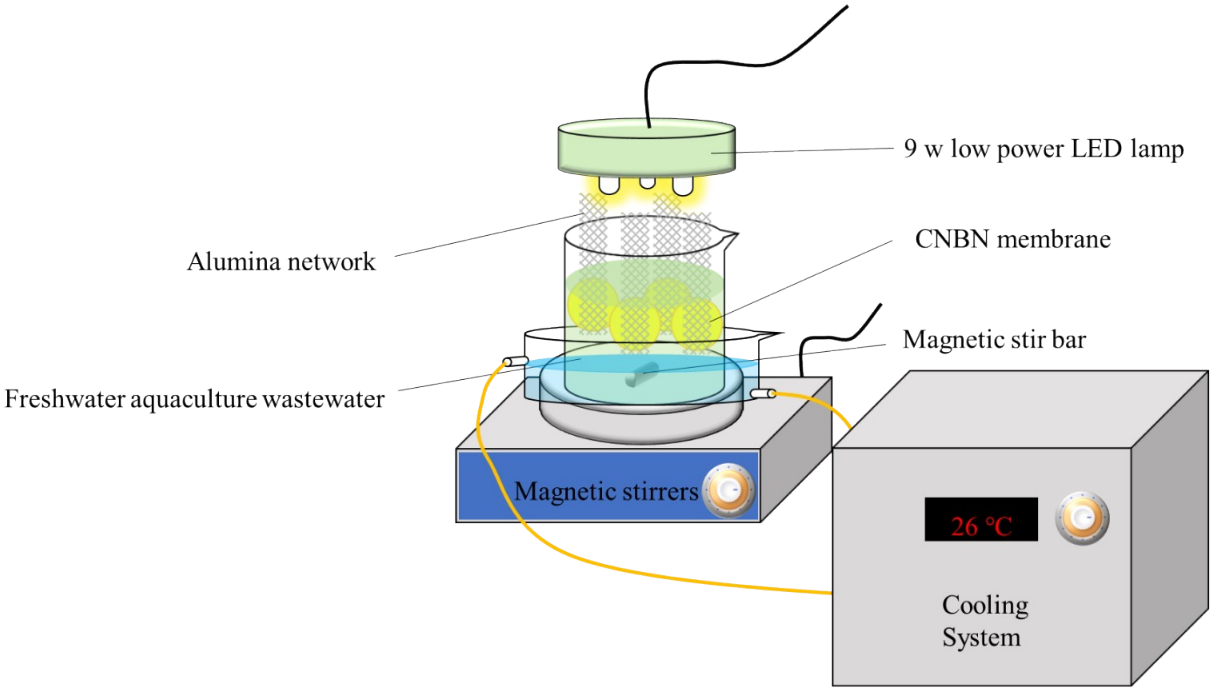

Figure S1. Reaction equipment

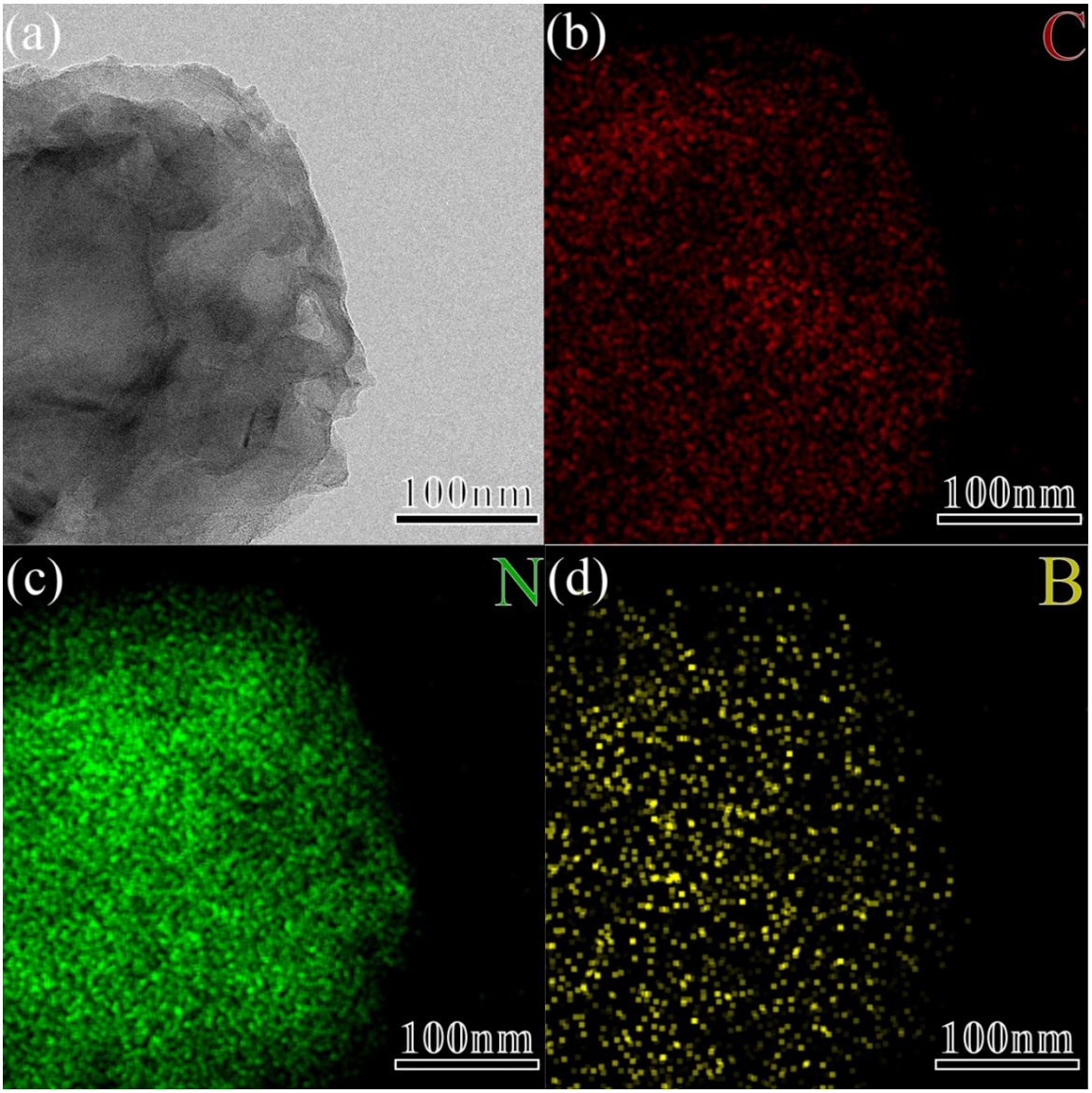

Figure S2. (a) TEM-EDS mapping of CNBN for (b) carbon, (c) nitrogen and (d) boron.

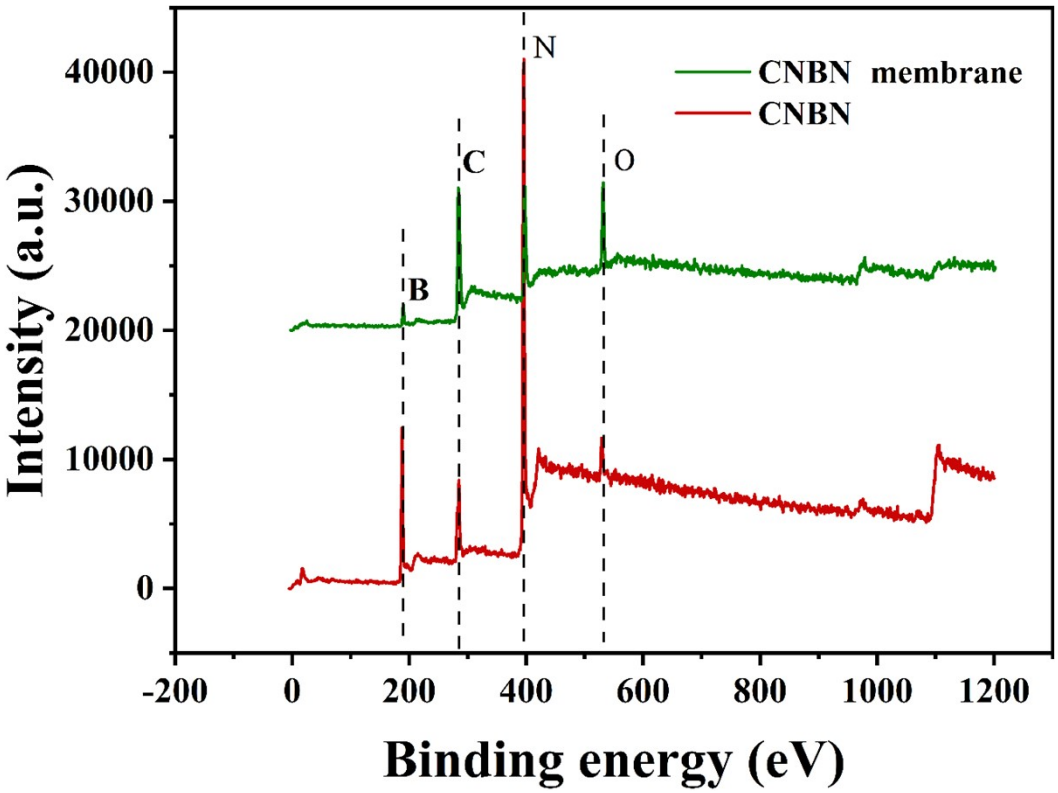

Figure S3. XPS scan spectra of CNBN membrane and CNBN.

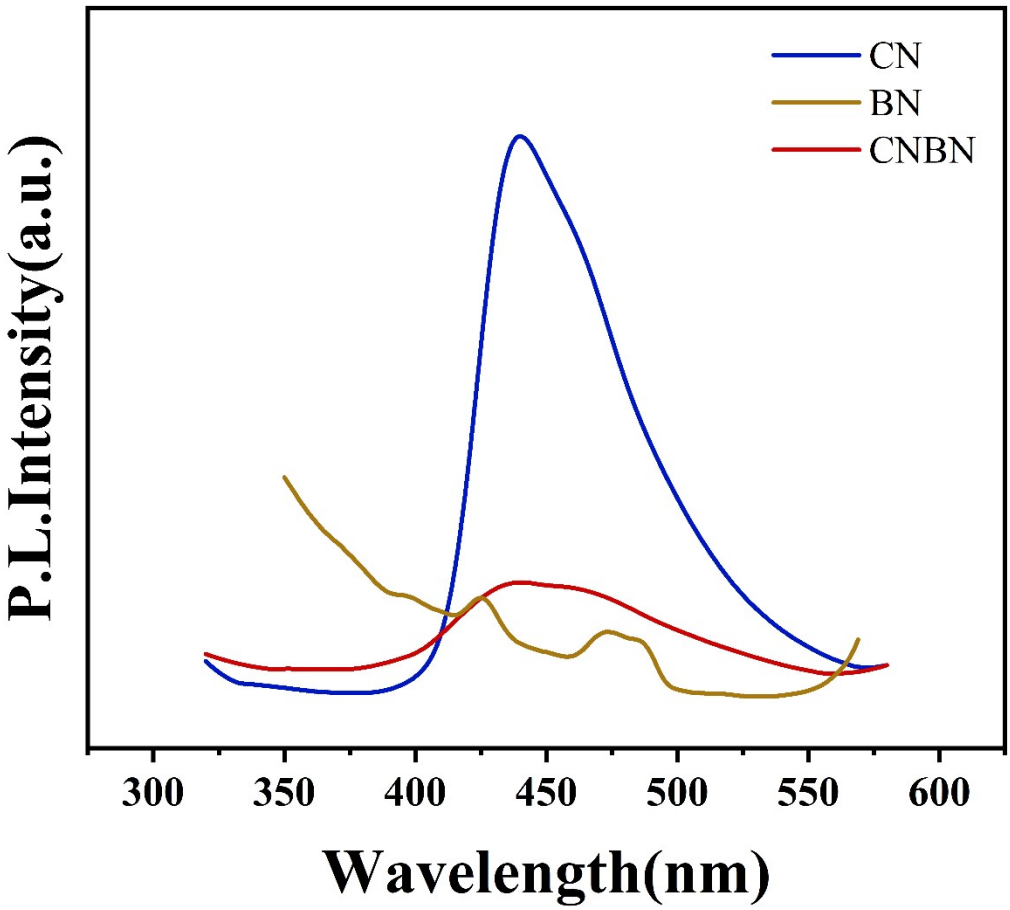

Figure S4. Fluorescence spectra of CN, BN and CNBN.

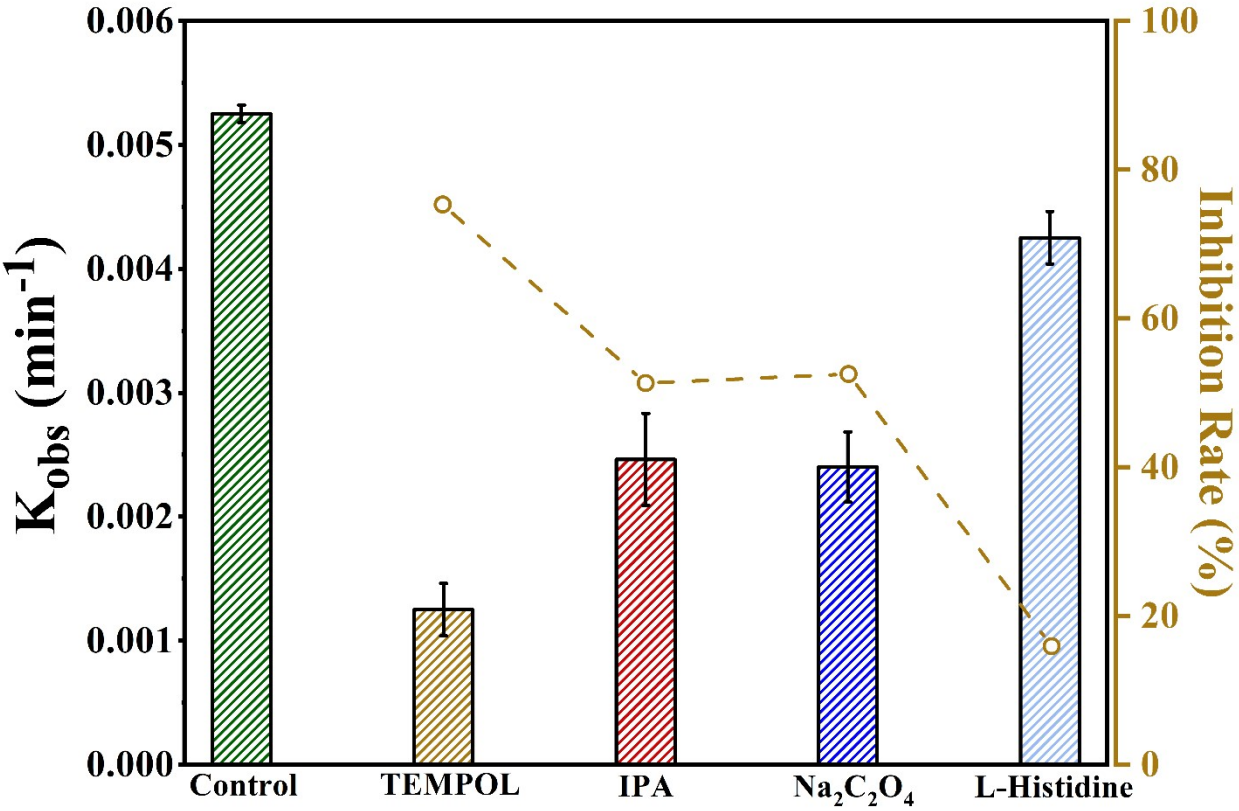

Figure S5. The degradation rate constants of CIP in the presence of scavengers. Four pieces of CNBN membranes, ultrapure water, [CIP]=10 mg L^{-1}, [optical power density]=5.71 mW cm^{-2}, pH=5.3.

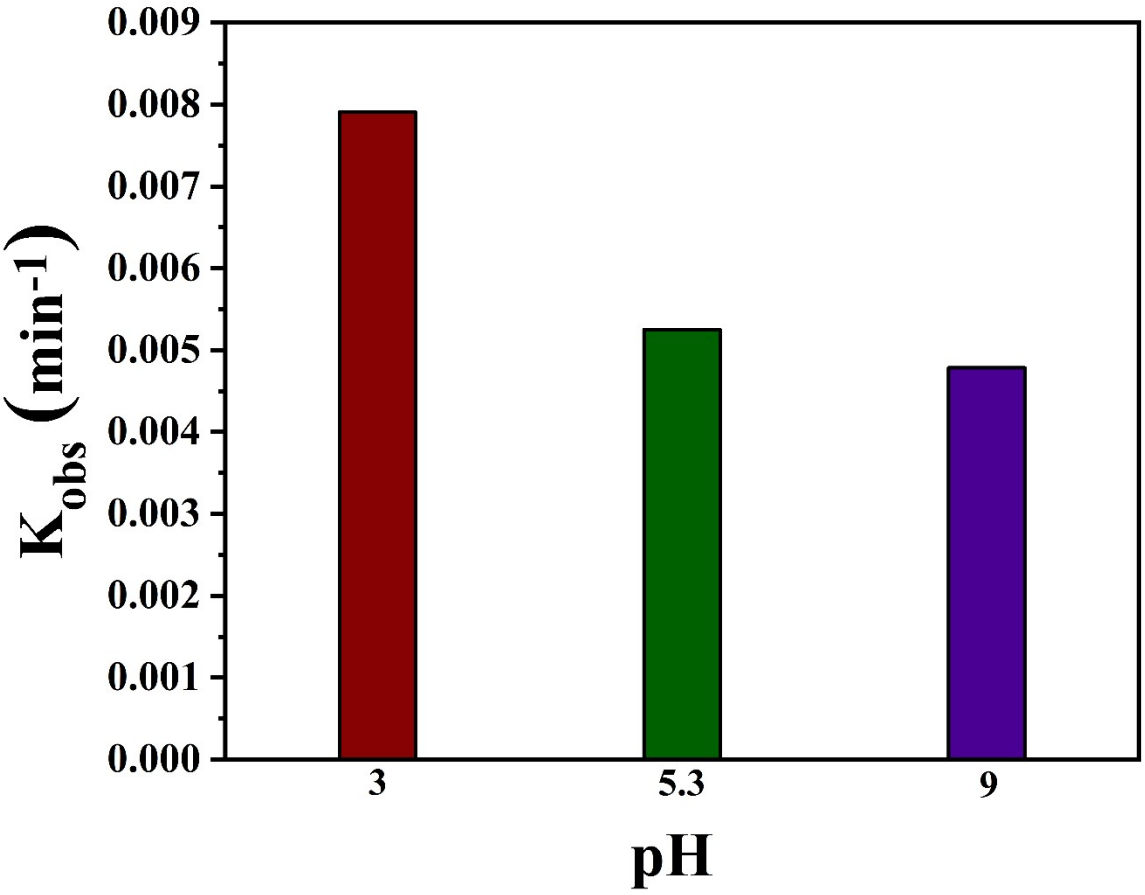

Figure S6. Influence of different initial pH on the degradation of CIP. Sulfuric acid and sodium hydroxide were used to adjust the initial pH while the control group did not adjust pH, four pieces of CNBN membranes, freshwater aquaculture wastewater, [CIP]=10 mg L^{-1}, [optical power density]=5.71 mW cm^{-2}, pH=5.3.

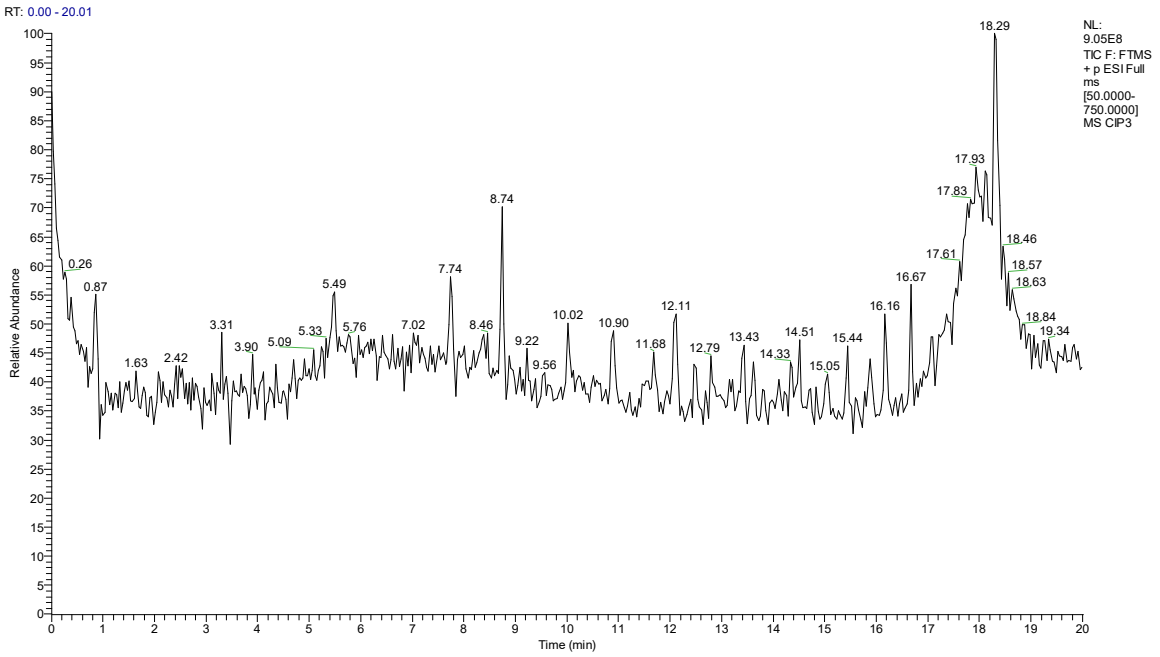

Figure S7. HPLC-MS/MS total ion current chromatogram of CIP.

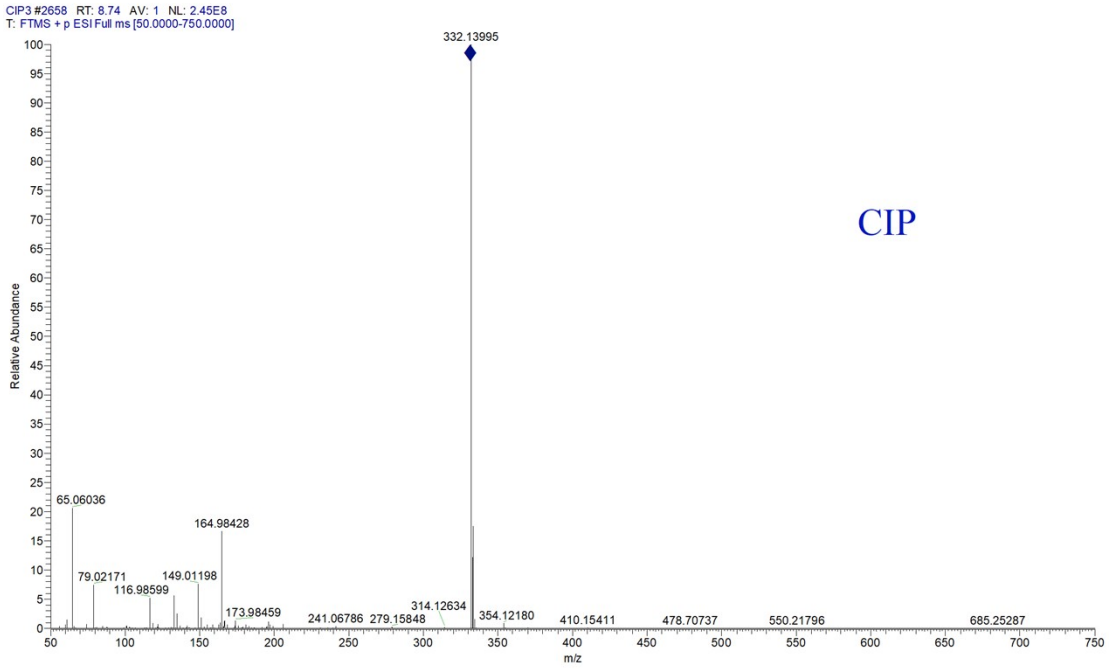
CIP3 #2658 RT: 8.74 AV: 1 NL: 2.45E8
T: FTMS + p ESI Full ms [50.0000-750.0000]
332.13995
CIP
Relative Abundance
m/z
65.06036
164.98428
79.02171
149.01198
116.98599
173.98459
241.06786
279.15848
314.12634
354.12180
410.15411
478.70737
550.21796
685.25287

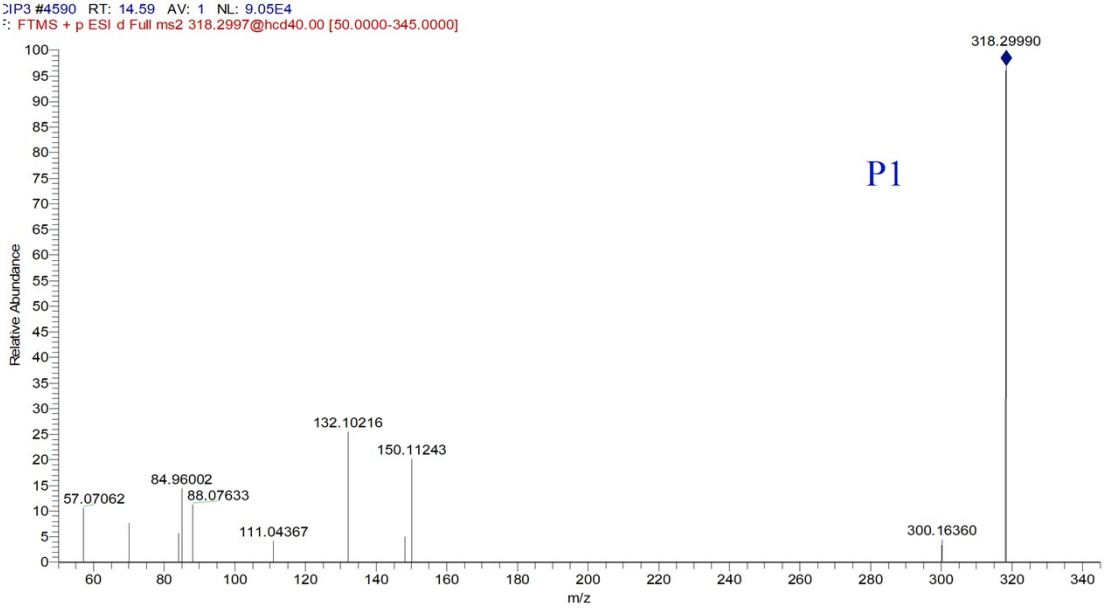
CIP3 #4590 RT: 14.59 AV: 1 NL: 9.05E4
F: FTMS + p ESI d Full ms2 318.2997@hcd40.00 [50.0000-345.0000]
318.29990
P1
Relative Abundance
m/z
132.10216
150.11243
84.96002
88.07633
57.07062
111.04367
300.16360

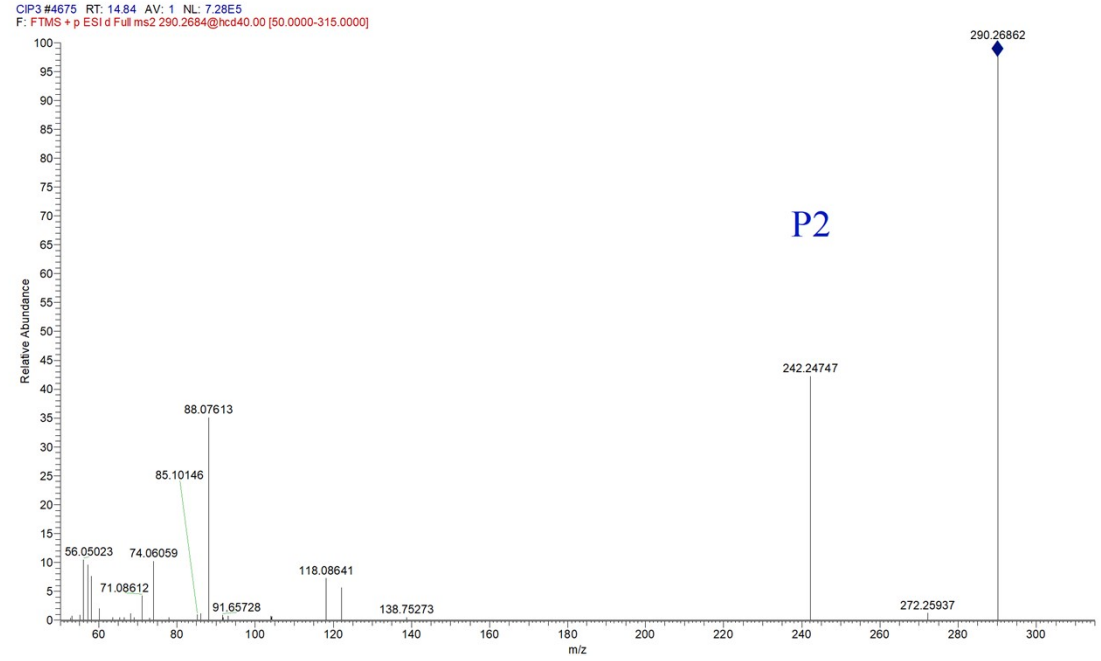
CIP3 #4675 RT: 14.84 AV: 1 NL: 7.28E5
F: FTMS + p ESI d Full ms2 290.2684@hcd40.00 [50.0000-315.0000]
P2
290.26862
242.24747
88.07613
85.10146
56.05023
74.06059
71.08612
118.08641
91.65728
138.75273
272.25937
Relative Abundance
m/z

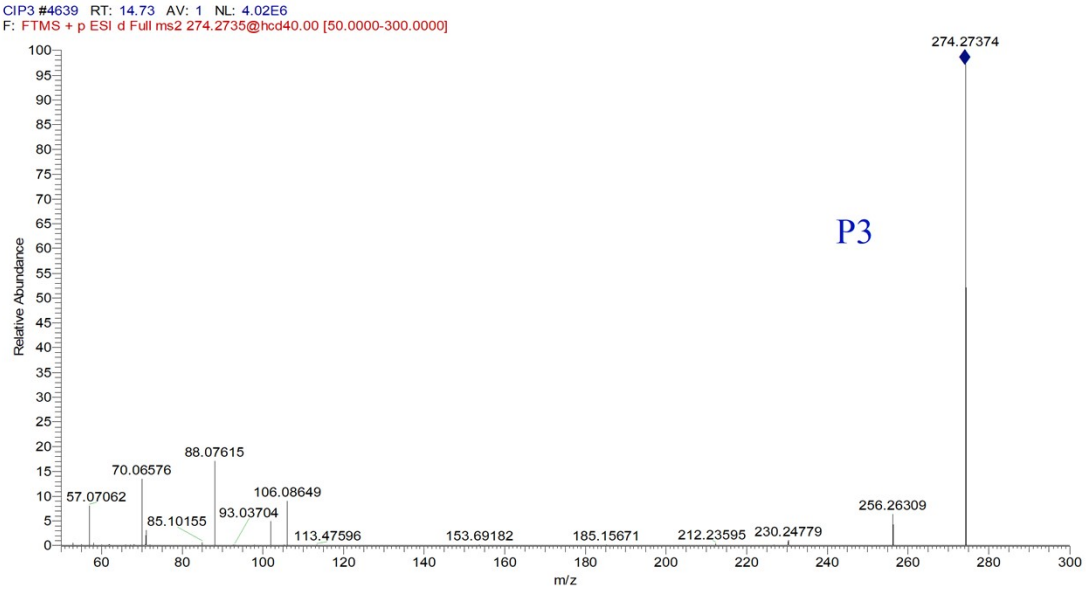
CIP3 #4639 RT: 14.73 AV: 1 NL: 4.02E6
F: FTMS + p ESI d Full ms2 274.2735@hcd40.00 [50.0000-300.0000]
P3
274.27374
88.07615
70.06576
57.07062
106.08649
93.03704
85.10155
256.26309
113.47596
153.69182
185.15671
212.23595
230.24779
Relative Abundance
m/z

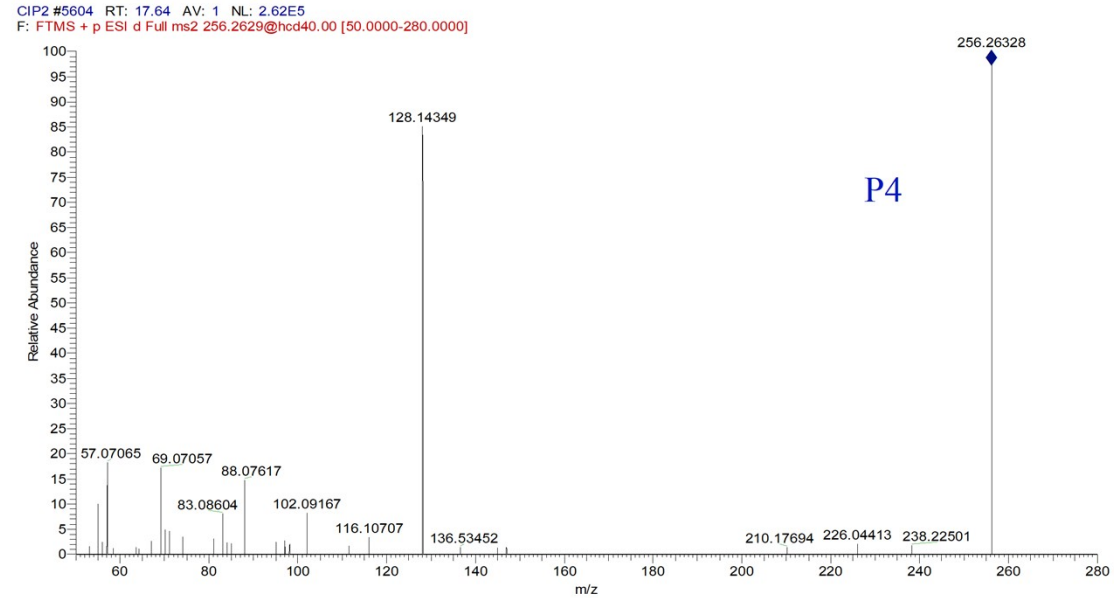
CIP2 #5604 RT: 17.64 AV: 1 NL: 2.62E5
F: FTMS + p ESI d Full ms2 256.2629@hcd40.00 [50.0000-280.0000]
P4
256.26328
128.14349
57.07065
69.07057
88.07617
83.08604
102.09167
116.10707
136.53452
210.17694
226.04413
238.22501
Relative Abundance
m/z

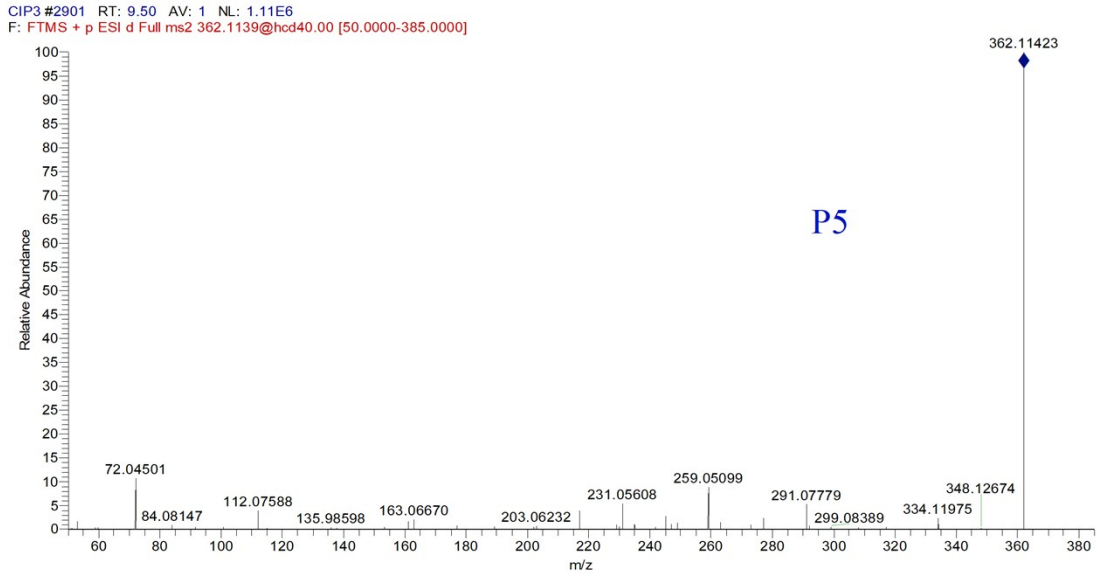
CIP3 #2901 RT: 9.50 AV: 1 NL: 1.11E6
F: FTMS + p ESI d Full ms2 362.1139@hcd40.00 [50.0000-385.0000]
P5
362.11423
72.04501
84.08147
112.07588
135.98598
163.06670
203.06232
231.05608
259.05099
291.07779
299.08389
334.11975
348.12674
Relative Abundance
m/z

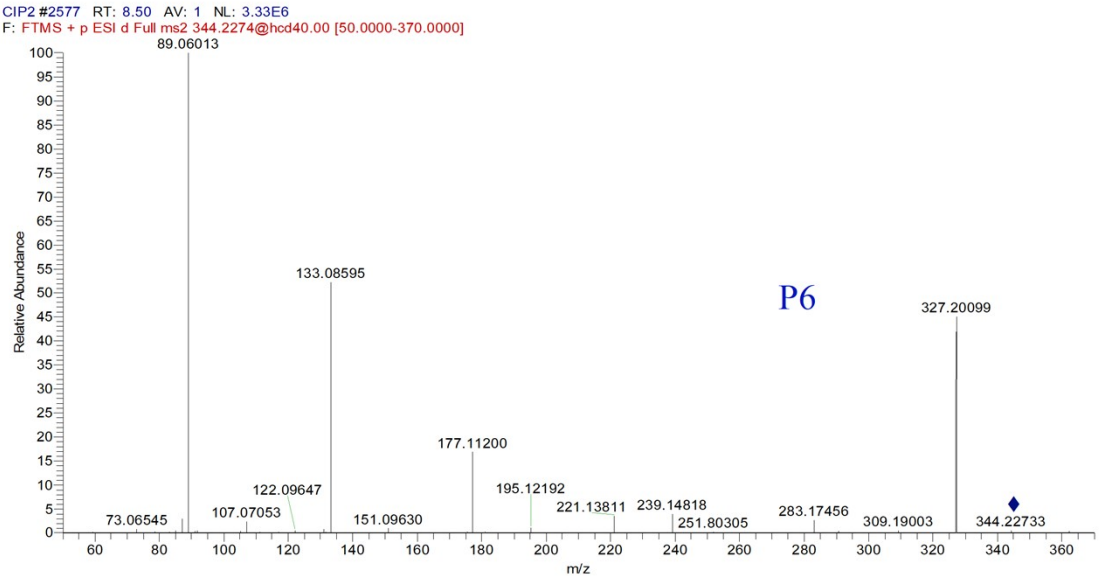
CIP2 #2577 RT: 8.50 AV: 1 NL: 3.33E6
F: FTMS + p ESI d Full ms2 344.2274@hcd40.00 [50.0000-370.0000]
P6
89.06013
73.06545
107.07053
122.09647
133.08595
151.09630
177.11200
195.12192
221.13811
239.14818
251.80305
283.17456
309.19003
327.20099
344.22733
Relative Abundance
m/z

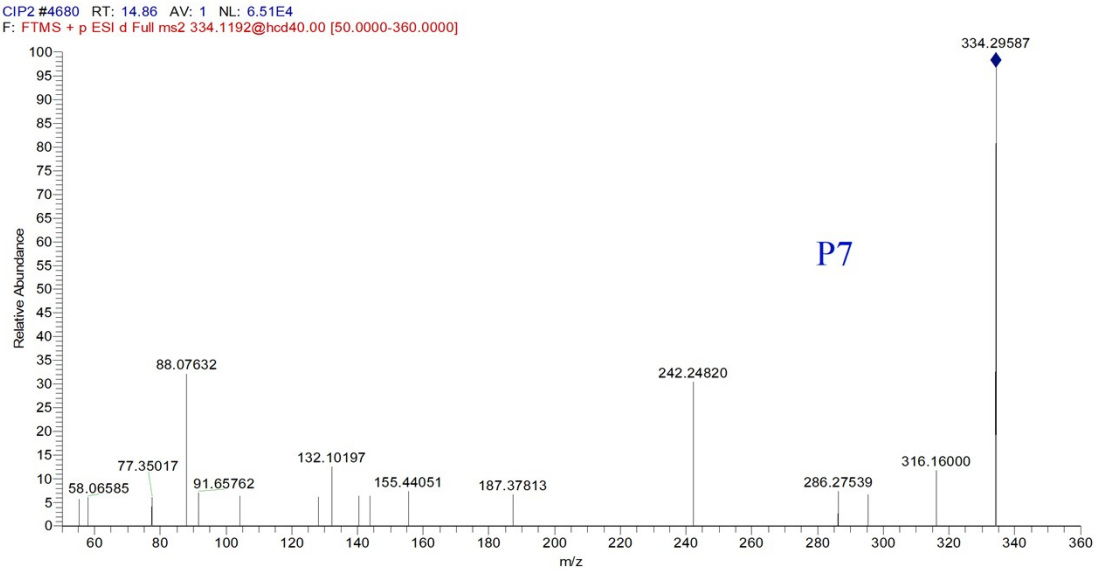
CIP2 #4680 RT: 14.86 AV: 1 NL: 6.51E4
F: FTMS + p ESI d Full ms2 334.1192@hcd40.00 [50.0000-360.0000]
P7
58.06585
77.35017
88.07632
91.65762
132.10197
155.44051
187.37813
242.24820
286.27539
316.16000
334.29587
Relative Abundance
m/z

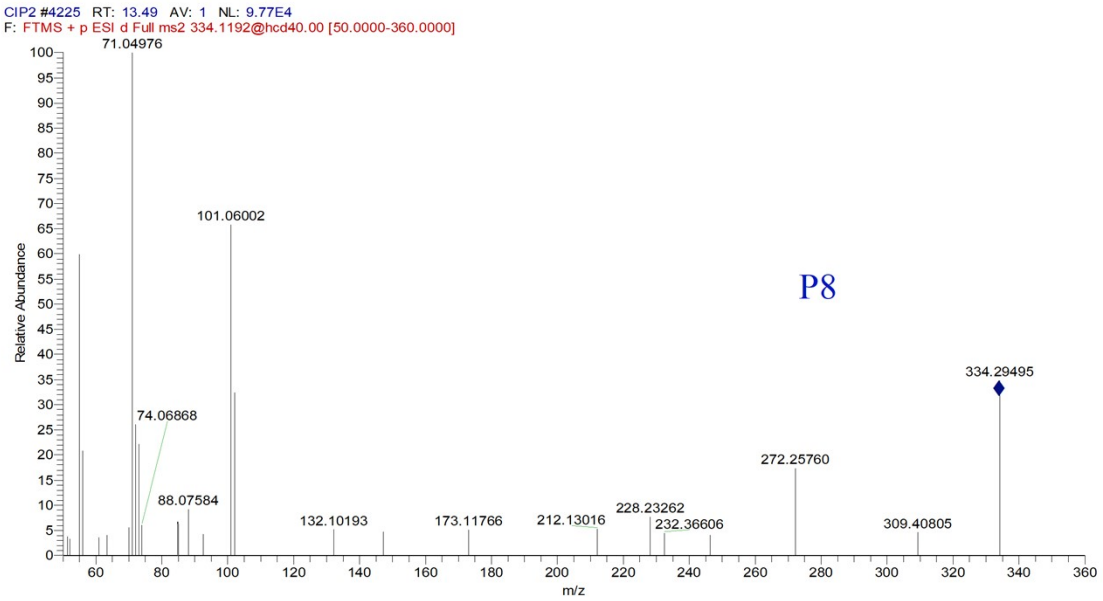
CIP2 #4225 RT: 13.49 AV: 1 NL: 9.77E4
F: FTMS + p ESI d Full ms2 334.1192@hcd40.00 [50.0000-360.0000]
71.04976
101.06002
74.06868
88.07584
132.10193
173.11766
212.13016
228.23262
232.36606
272.25760
309.40805
334.29495
P8
Relative Abundance
m/z

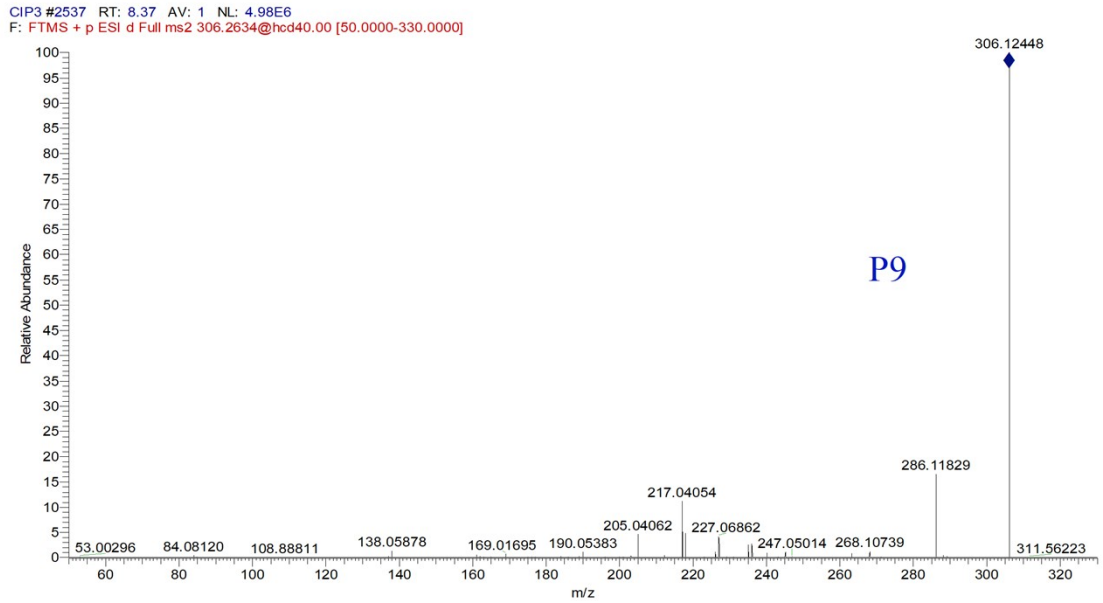
CIP3 #2537 RT: 8.37 AV: 1 NL: 4.98E6
F: FTMS + p ESI d Full ms2 306.2634@hcd40.00 [50.0000-330.0000]
306.12448
286.11829
217.04054
205.04062
227.06862
53.00296
84.08120
108.88811
138.05878
169.01695
190.05383
247.05014
268.10739
311.56223
P9
Relative Abundance
m/z

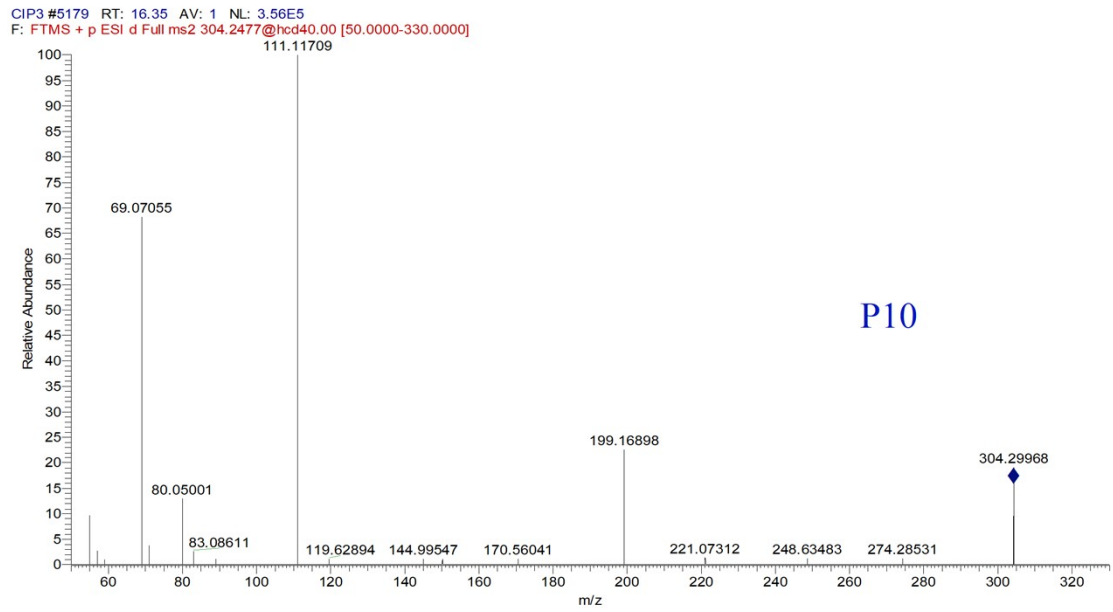
CIP3 #5179 RT: 16.35 AV: 1 NL: 3.56E5
F: FTMS + p ESI d Full ms2 304.2477@hcd40.00 [50.0000-330.0000]
111.11709
69.07055
199.16898
304.29968
80.05001
83.08611
119.62894
144.99547
170.56041
221.07312
248.63483
274.28531
P10
Relative Abundance
m/z

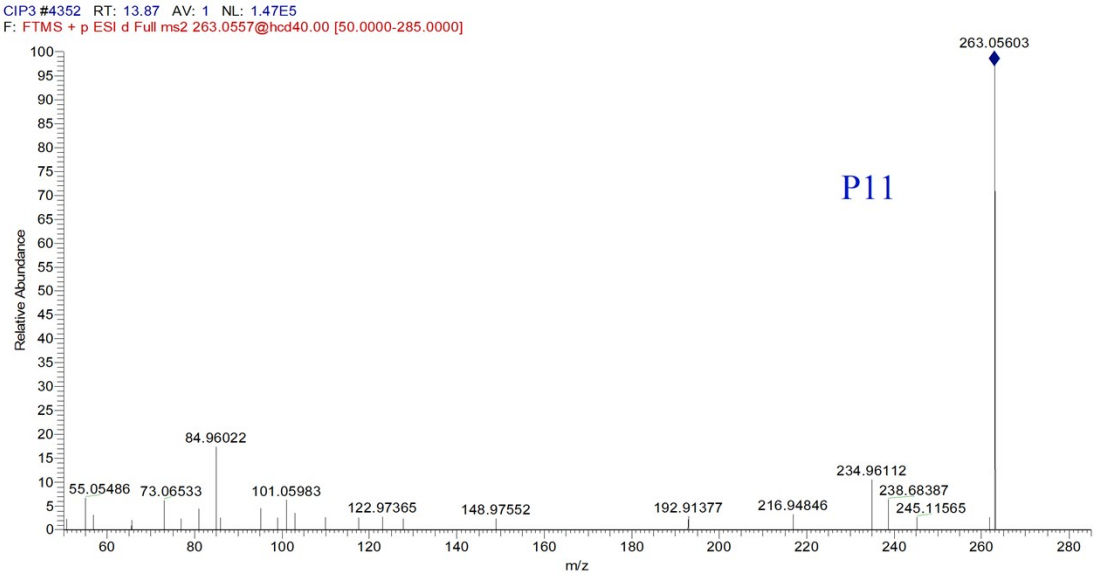
CIP3 #4352 RT: 13.87 AV: 1 NL: 1.47E5
F: FTMS + p ESI d Full ms2 263.0557@hcd40.00 [50.0000-285.0000]
263.05603
P11
84.96022
234.96112
55.05486
73.06533
101.05983
122.97365
148.97552
192.91377
216.94846
238.68387
245.11565
Relative Abundance
m/z

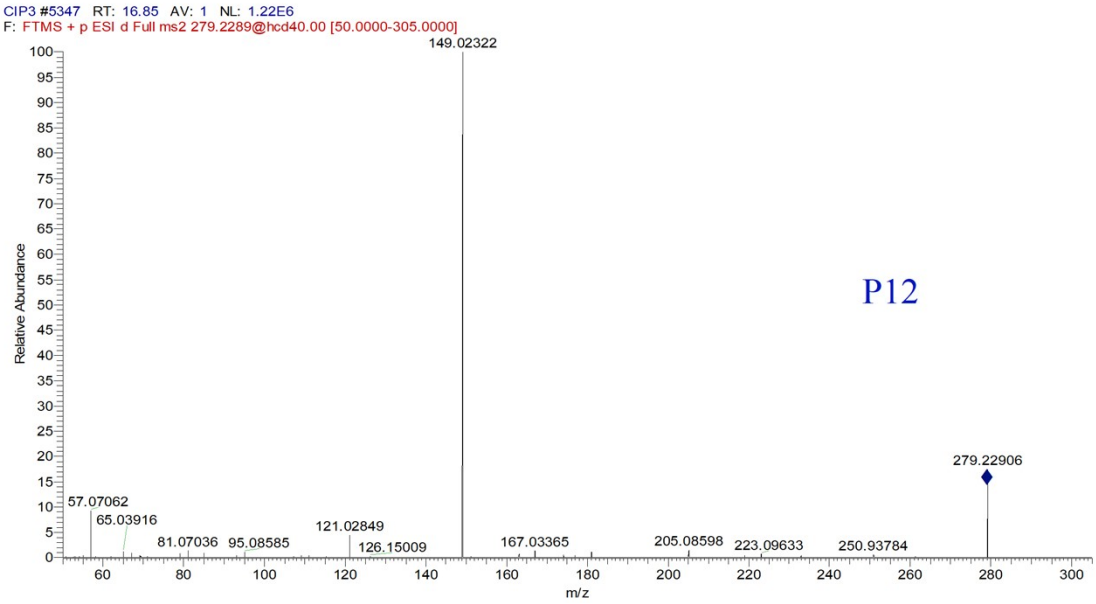
CIP3 #5347 RT: 16.85 AV: 1 NL: 1.22E6
F: FTMS + p ESI d Full ms2 279.2289@hcd40.00 [50.0000-305.0000]
149.02322
P12
279.22906
57.07062
65.03916
81.07036
95.08585
121.02849
126.15009
167.03365
205.08598
223.09633
250.93784
Relative Abundance
m/z

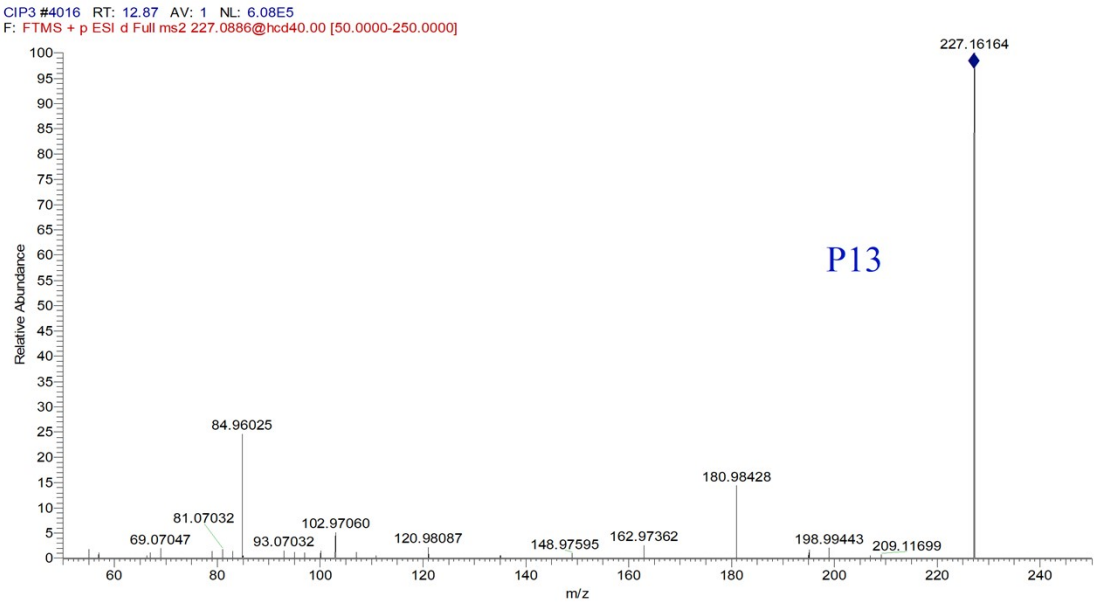
CIP3 #4016 RT: 12.87 AV: 1 NL: 6.08E5
F: FTMS + p ESI d Full ms2 227.0886@hcd40.00 [50.0000-250.0000]
227.16164
P13
84.96025
180.98428
81.07032
69.07047
93.07032
102.97060
120.98087
148.97595
162.97362
198.99443
209.11699
Relative Abundance
m/z

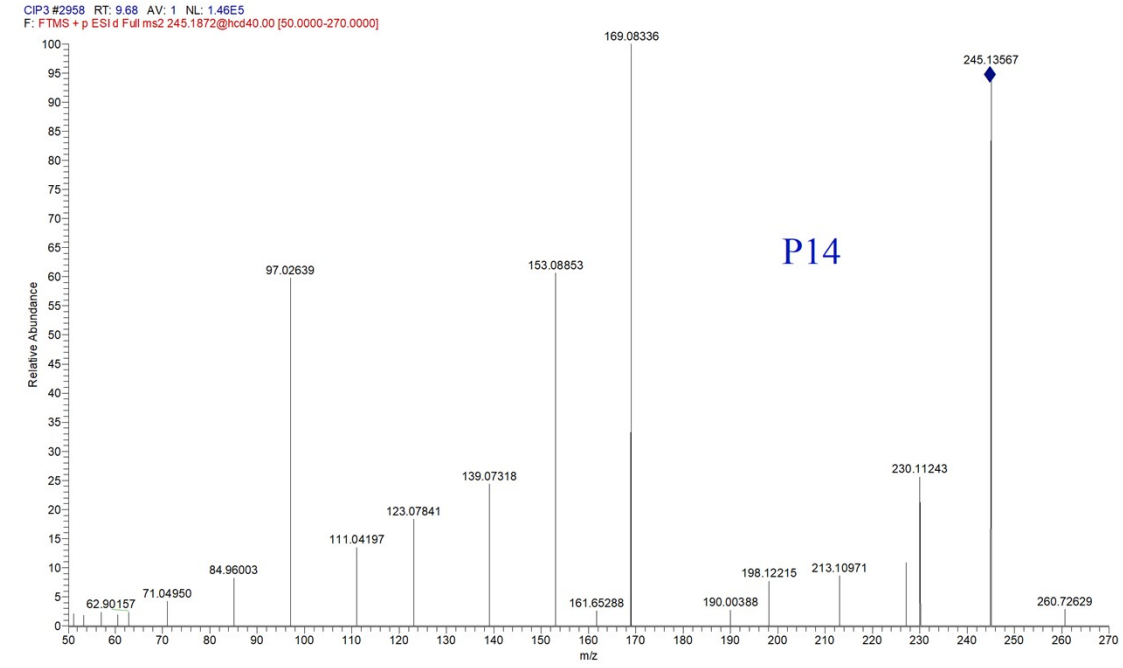
CIP3 #2958 RT: 9.68 AV: 1 NL: 1.46E5
F: FTMS + p ESI d Full ms2 245.1872@hcd40.00 [50.0000-270.0000]
P14
Relative Abundance
m/z
169.08336
245.13567
97.02639
153.08853
139.07318
230.11243
123.07841
111.04197
84.96003
198.12215
213.10971
71.04950
62.90157
161.65288
190.00388
260.72629

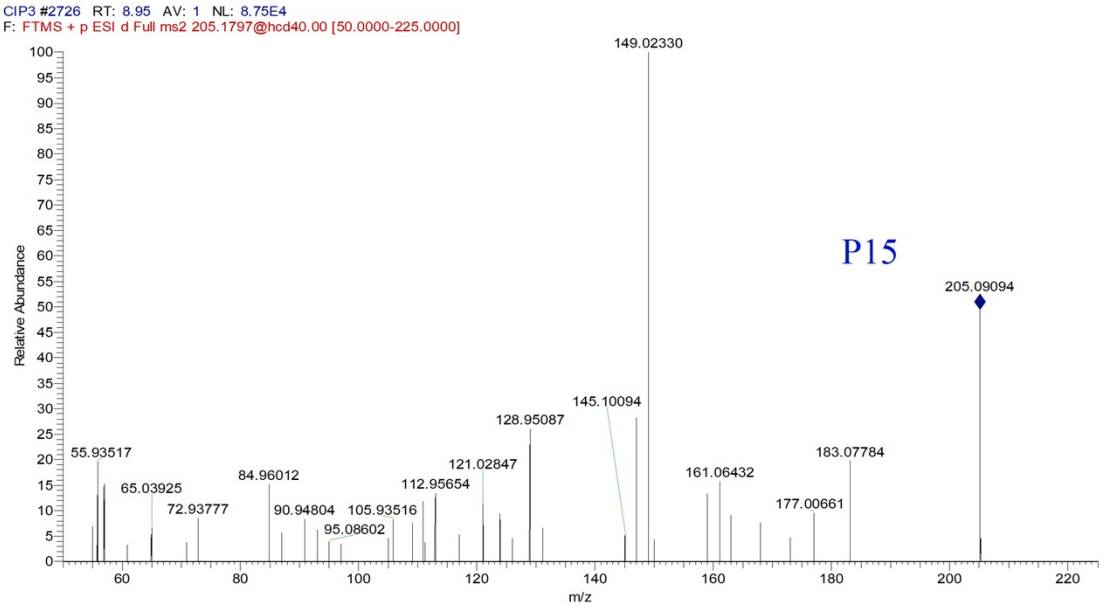
CIP3 #2726 RT: 8.95 AV: 1 NL: 8.75E4
F: FTMS + p ESI d Full ms2 205.1797@hcd40.00 [50.0000-225.0000]
P15
Relative Abundance
m/z
149.02330
205.09094
145.10094
128.95087
55.93517
121.02847
183.07784
84.96012
161.06432
65.03925
112.95654
177.00661
72.93777
90.94804
105.93516
95.08602

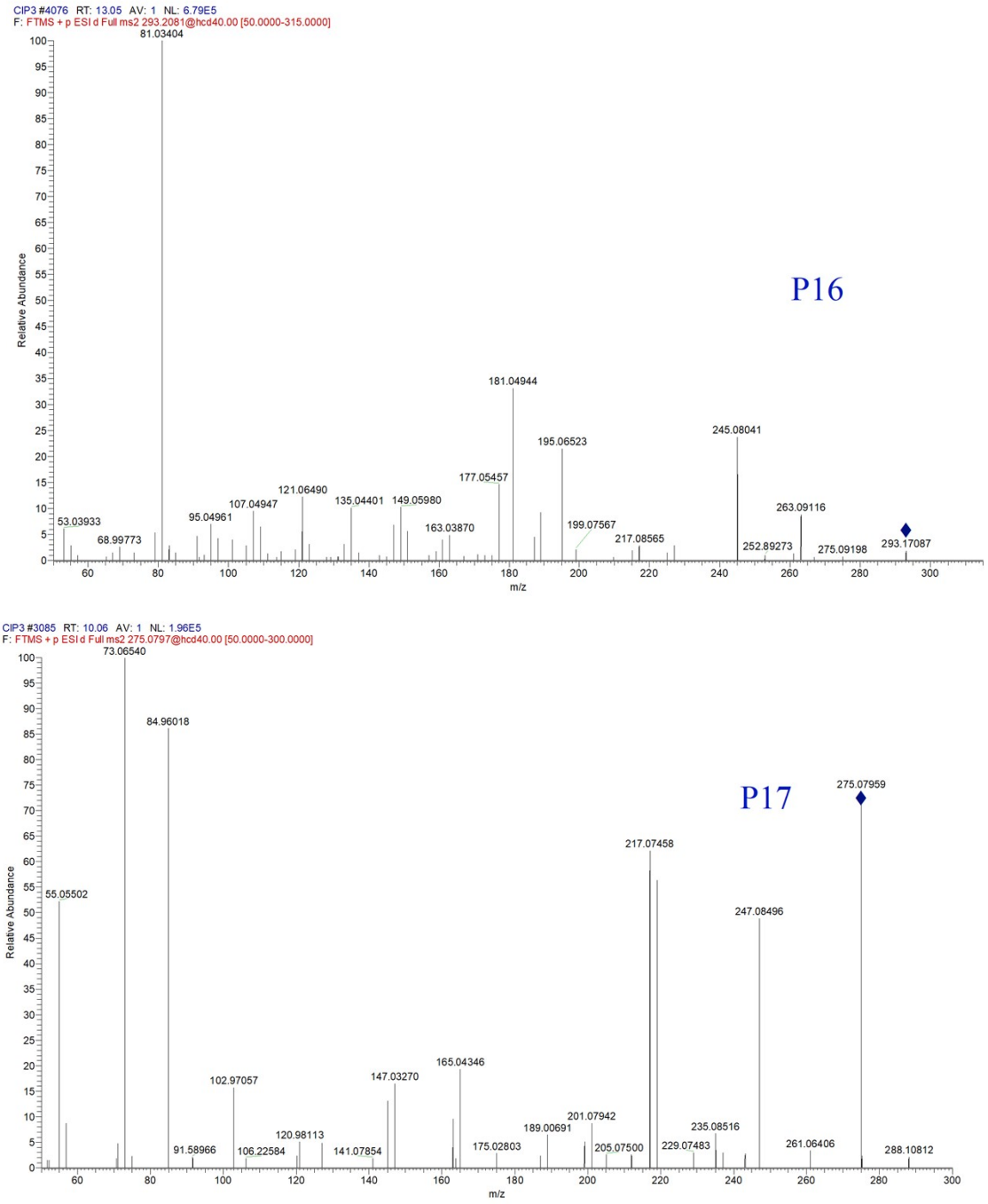

Figure S8. MS/MS fragmentation information of the observed transformation products (P1-P17), the blue diamond represents the corresponding parent ion.

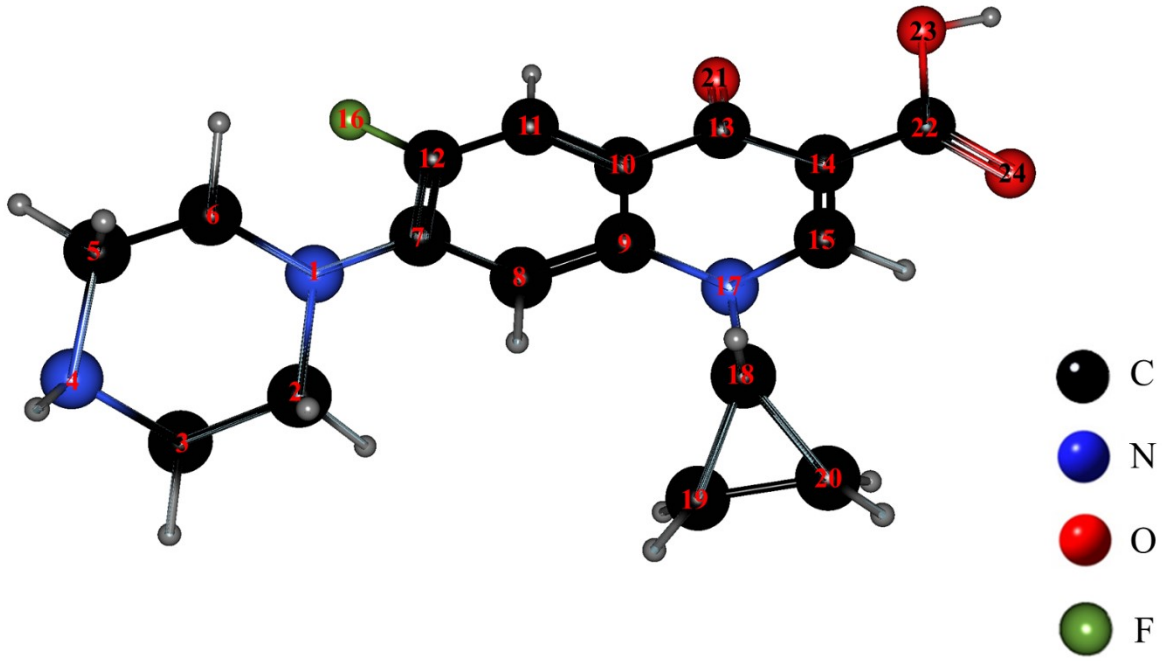

Figure S9. Atomic numbering of CIP used for FEDs analysis and discussion of reaction sites [3].

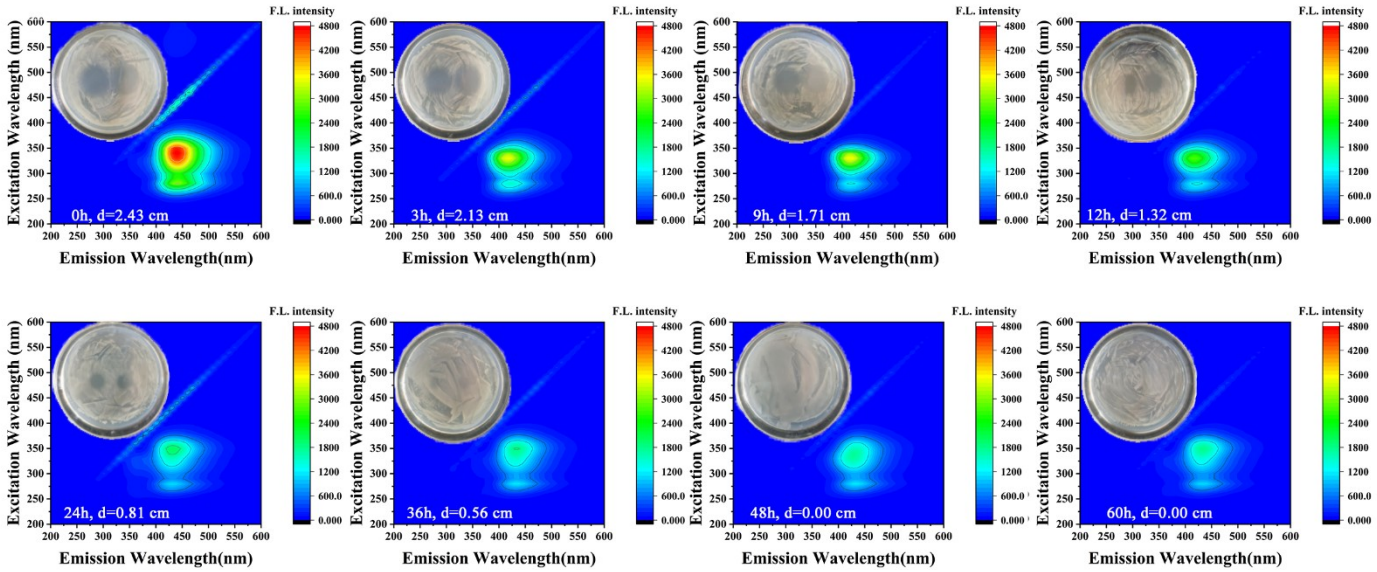

Figure S10. 3D-EEM images and antibiotic residue of CIP (*E. coli* was used as an indicator) of CIP treated solution that photocatalytic degraded. The decreasing drug sensitive ring on agar plate in the figure represents the disappearance of antibiotic residues over time. The time of the reaction and the diameter of the drug sensitive ring on agar plate were marked in white words in each image. Four pieces of CNBN membranes, ultrapure water, [CIP]=10 mg L^{-1}, [optical power density]=5.71 mW cm^{-2}, pH=5.3.

.

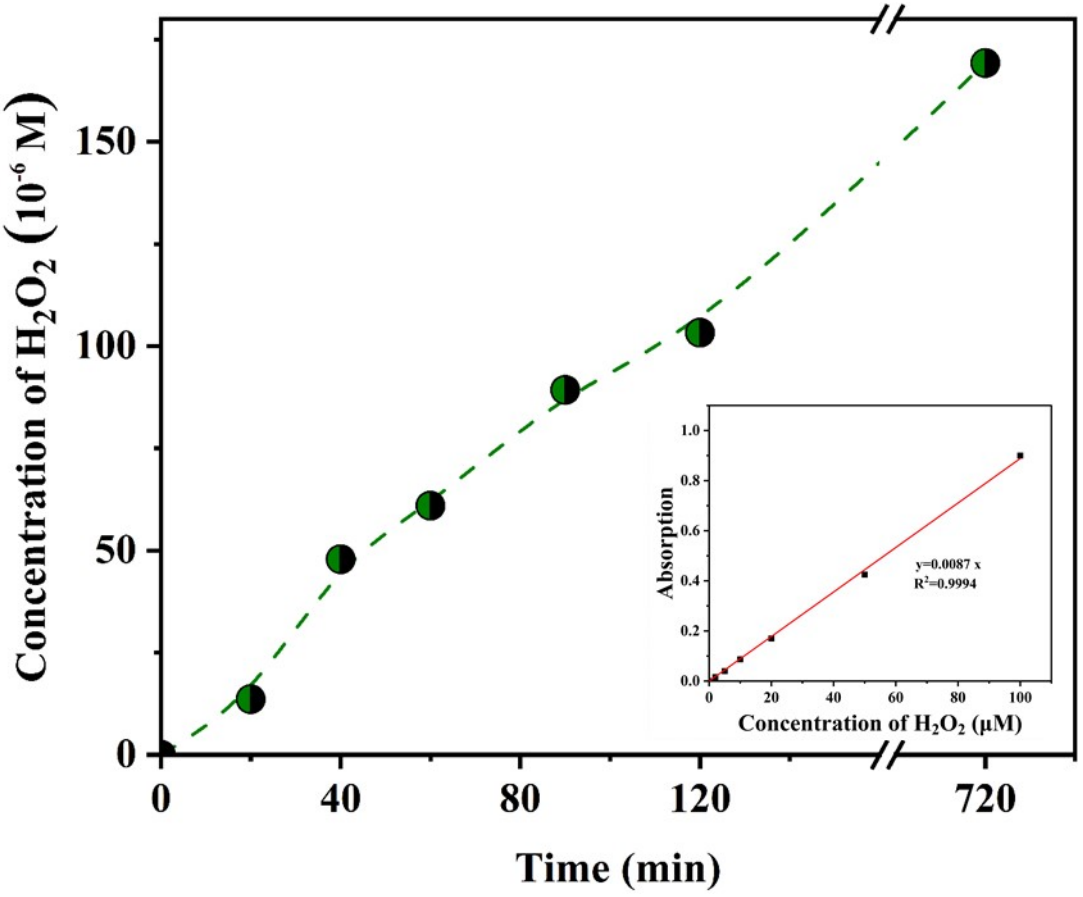

Figure S11. CNBN membrane for the photocatalytic H_2O_2 production (embedded figure is the UV absorption standard curve of H_2O_2). Four pieces of CNBN membranes, ultrapure water, [CIP]=10 mg L^{-1}, [optical power density]=5.71 mW cm^{-2}, pH=5.3.

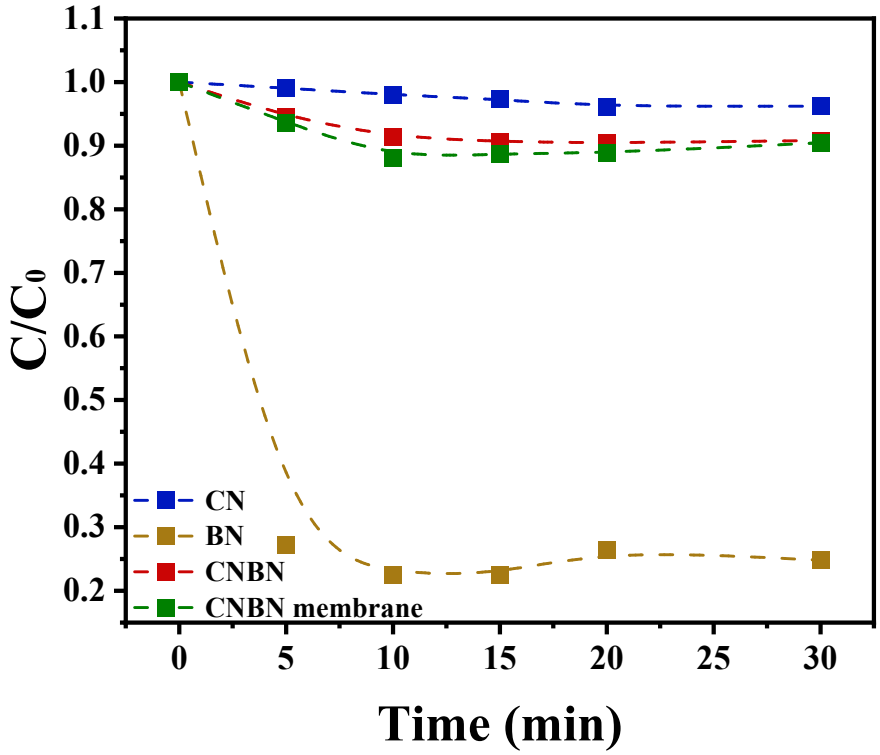

Figure S12. The adsorption equilibrium time of CIP with powder CN, powder BN, powder CNBN and CNBN membrane in dark, powder catalysts concentration= 900 mg L^{-1}, four pieces of CNBN membranes, freshwater aquaculture wastewater, [CIP]=10 mg L^{-1}, pH=5.3.

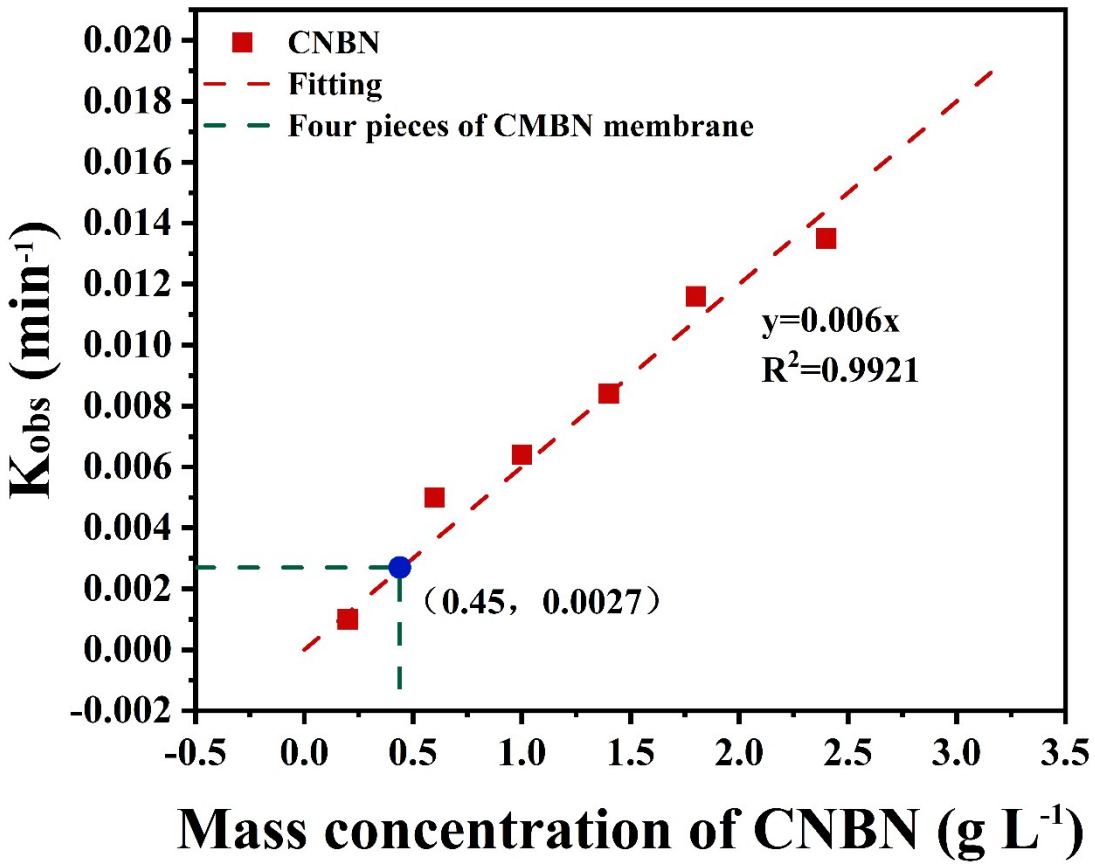

Figure S13. Photocatalytic degradation rate of CIP at different powder CNBN concentrations in freshwater aquaculture wastewater, four pieces of CNBN membranes, freshwater aquaculture wastewater, [CIP]=10 mg L^{-1}, [optical power density]= 5.71 mW cm^{-2}, pH=5.3.

References

1. C. Kormann, D. W. Bahnemann and M. R. Hoffmann, Photocatalytic production of hydrogen peroxides and organic peroxides in aqueous suspensions of titanium dioxide, zinc oxide, and desert sand, *Environmental Science & Technology*, 1988, **22**, 798-806.
2. D. Li, C. Wen, J. Huang, J. Zhong, P. Chen, H. Liu, Z. Wang, Y. Liu, W. Lv and G. Liu, High-efficiency Ultrathin Porous Phosphorus-Doped Graphitic Carbon Nitride Nanosheet Photocatalyst for Energy Production and Environmental Remediation, *Applied Catalysis B: Environmental*, 2022, DOI: https://doi.org/10.1016/j.apcatb.2022.121099, 121099.
3. F. Wang, Y. Feng, P. Chen, Y. Wang, Y. Su, Q. Zhang, Y. Zeng, Z. Xie, H. Liu, Y. Liu, W. Lv and G. Liu, Photocatalytic degradation of fluoroquinolone antibiotics using ordered mesoporous g-C_3N_4 under simulated sunlight irradiation: Kinetics, mechanism, and antibacterial activity elimination, *Applied Catalysis B: Environmental*, 2018, **227**, 114-122.